Academic Science

International Journal of Computer & Mathematical Sciences
IJCMS
ISSN 2347 – 8527
Volume 3, Issue 1
April 2014

Penetrative convection via internal heating in superposed fluid and anisotropic porous layers with throughflow

Gangadharaiah, Y. H., Suma, S. P., Nagarathnamma. H

Abstract. The onset of thermal convection due to heating from below in a system consisting of a fluid layer overlying a porous layer with anisotropic permeability and thermal diffusivity is studied. The onset of penetrative convection simulated via internal heating in the presence of a vertical throughflow. Flow in the porous medium is governed by Forchheimer-extended Darcy equation and the Beavers–Joseph slip condition is applied at the interface between the fluid and the porous layers. The boundaries are considered to be rigid, however permeable, and insulated to temperature perturbations. The eigen value problem is solved using a regular perturbation technique with wave number as a perturbation parameter. It is found that the depth of the relative layers, the direction of throughflow, the presence of volumetric internal heat source in fluid and/or porous layer and mechanical and thermal anisotropy parameters have a profound effect on the stability of the system. Decreasing the mechanical anisotropy parameter and increasing the thermal anisotropy parameter leads to stabilization of the system. Besides, the possibility of control of thermal convection by suitable choice of physical parameters is discussed in detail.

Key words: composite layer; penetrative convection; throughflow.

Gangadharaiah, Y. H.
Department of Mathematics, New Horizon College of Engineering, Bangalore-560 103, India

E-mail address: gangu.honnappa@gmail.com

Suma, S. P
Department of Mathematics, Cambridge Institute of Technology,Bangalore-560 036, India

Nagarathnamma. H
Department of Mathematics, Ambedkar Institute of Technology, Bangalore, India

Academic Science

International Journal of Computer & Mathematical Sciences
IJCMS
ISSN 2347 – 8527
Volume 3, Issue 1
April 2014

Nomenclature

a	horizontal wave number, $\sqrt{l^2+m^2}$
A	ratio of heat capacities
D	differential operator d/dz
d	thickness of the fluid layer
d_m	thickness of the porous layer
Da	Darcy number k/d_m^2
$\vec{g}$	acceleration due to gravity
k	permeability
l,m	wave number in x and y-directions respectively
R	Rayleigh number in the fluid layer $\alpha g\ (T_0-T_u)\ d^3/\nu\kappa$
R_m	Rayleigh number in a porous medium $\alpha g\ (T_l-T_0)\ d_m k/\nu\kappa_m$
p	pressure
Pr	Prandtl number for fluid layer, ν/κ
Pr_m	porous medium Prandtl number, $\nu\phi/\kappa_m$
Pe	throughflow dependent Peclet number for fluid layer, $W_0 d/\kappa$
Pe_m	through flow dependent Peclet number for a porous medium, $W_0 d_m/\kappa_m$
T	temperature
T_0	temperature at the interface
$\vec{V}$	velocity vector (u, v, w)
W	amplitude of perturbed vertical velocity
q_f	heat source in the fluid layer
q_m	heat source in the porous layer
Ns_f	dimensionless heat source in the fluid layer $q_f d^2/2\kappa\ (T_0-T_u)$

International Journal of Computer & Mathematical Sciences
IJCMS
ISSN 2347 – 8527
Volume 3, Issue 1
April 2014

Ns_m dimensionless heat source in the porous layer $q_m d_m^2 / 2\kappa_m \ T_l - T_0$

Greek symbols

β slip parameter

∇_h^2 horizontal Laplacian operator $\nabla_h^2 = \partial^2/\partial x^2 + \partial^2/\partial y^2$

∇^2 Laplacian operator $\nabla^2 = \partial^2/\partial x^2 + \partial^2/\partial y^2 + \partial^2/\partial z^2$

ε_T ratio of thermal diffusivities κ/κ_m

ϕ porosity of the porous medium

κ thermal diffusivity

Θ amplitude of perturbed temperature

μ fluid viscosity

ρ_0 fluid density

ξ mechanical anisotropy parameter K_h / K_v

χ thermal anisotropy parameter $\kappa_{mh} / \kappa_{mv}$

σ temperature dependent surface tension

v kinematic viscosity μ/ρ_0

ζ depth ratio d/d_m

Subscripts

b basic state

l lower

m porous medium

u upper

1 Introduction

The problem of fluid flow over a porous medium is encountered in a wide range of industrial and geophysical applications, such as flows in fuel cells, filtration processes, the extraction of oil

International Journal of Computer & Mathematical Sciences
IJCMS
ISSN 2347 – 8527
Volume 3, Issue 1
April 2014

from underground reservoirs, ground-water pollution, the manufacture of composite materials, and in flow in biological materials, see e.g. Allen (1984), Hill and Straughan (2009), Nield and Bejan (2006).

A linear stability analysis of the convective instability in superposed horizontal fluid and porous layers with throughflow in the vertical direction for isothermal boundaries has been implemented by Chen (1990). It is found that in such a physical configuration both stabilizing and destabilizing factors due to vertical throughflow can be enhanced so that a more precise control of the buoyantly driven instability in either a fluid or a porous layer is possible. Khalili et al. (2003) have investigated the effect of throughflow on thermal convective instability in superposed fluid and porous layers system for the boundaries insulated to temperature perturbations and an analytical expression for the critical Rayleigh number is obtained. Carr and Straughan (2003) have considered penetrative convection in the porous-medium–fluid system by employing a quadratic equation of state, while Carr (2004) has studied penetrative convection via internal heating in a composite two-layer system in which a layer of fluid overlies and saturates a layer of isotropic porous medium. Shivakumara et al. (2011)have investigated the criterion for the onset of surface tension-driven convection in the presence of temperature gradients in a two-layer system comprising a fluid saturated anisotropic porous layer over which lies a layer of fluid while the effect of internal heating on the problem has been considered by Shivakumara et al. (2012).

The problem we wish to investigate is one of thermal convection in a system consisting of a anisotropic porous layer underlying a fluid layer where there is throughflow through the system. In addition, we intend focusing attention on the system heated internally in both fluid and anisotropic porous layers, thereby incorporating penetrative convection. One way in which penetrative convection with throughflow in composite fluid and porous layers system may be important for industrial application is that it yields a potential method of controlling the onset and behavior of convection. To be able to know how to control convection, one needs to determine when the convection sets in.

Academic Science

International Journal of Computer & Mathematical Sciences
IJCMS
ISSN 2347 – 8527
Volume 3, Issue 1
April 2014

The intent of the present study is to obtain the criterion for the onset of penetrative convection via internal heating in a two-layer system in which a fluid layer overlies a layer of fluid saturated anisotropic porous medium in the presence of vertical throughflow. The boundaries are considered to be insulated to temperature perturbations. A regular perturbation technique with wave number as a perturbation parameter is used to solve the eigen value problem in a closed form .A wide-ranging parametric study is undertaken to explore their impact on the stability characteristics of the system.

2 Mathematical Formulation

We consider penetrative convection via internal heating in a system consisting of an infinite horizontal fluid layer of thickness d overlying a layer of Darcy porous medium of thickness d_m with throughflow of constant vertical velocity W_0 as shown in Fig. 1. A Cartesian coordinate system (x, y, z) is chosen with the origin at the interface and the z-axis vertically upward. The gravity acts in the vertical direction with constant acceleration g. The top and bottom boundaries are assumed to be rigid-permeable and are maintained at uniform but different temperatures T_l and $T_u (< T_l)$ respectively.

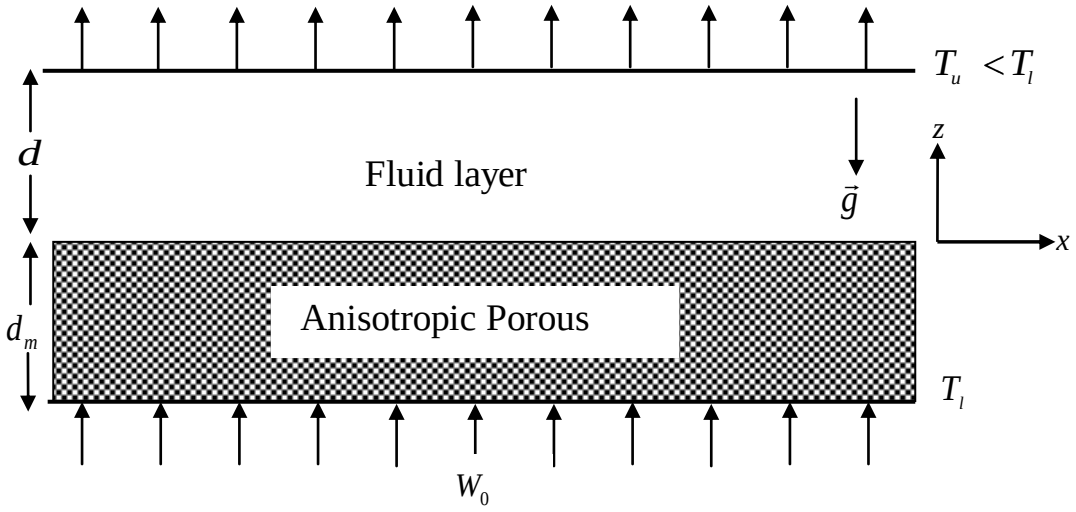

Fig. 1 Physical configuration

International Journal of Computer & Mathematical Sciences
IJCMS
ISSN 2347 – 8527
Volume 3, Issue 1
April 2014

The governing equations for the fluid and the porous layers are:

Fluid layer:

$$\nabla \cdot \vec{V} = 0 \tag{1}$$

$$\rho_0 \left[\frac{\partial \vec{V}}{\partial t} + \vec{V} \cdot \nabla \vec{V} \right] = -\nabla p + \rho_0 \vec{g} \left[1 - \alpha \left(T - T_0 \right) \right] + \mu \nabla^2 \vec{V} \tag{2}$$

$$\frac{\partial T}{\partial t} + \vec{V} \cdot \nabla T = \kappa \nabla^2 T + q . \tag{3}$$

Porous layer:

$$\nabla \cdot \vec{V}_m = 0 \tag{4}$$

$$\frac{\rho_0}{\phi} \frac{\partial \vec{V}_m}{\partial t} = -\nabla p_m + \rho_0 \vec{g} \left[1 - \alpha \left(T_m - T_0 \right) \right] - \mu \underset{\sim}{K}^{-1} \cdot \vec{V}_m \tag{5}$$

$$A \frac{\partial T_m}{\partial t} + \vec{V}_m \cdot \nabla_m T_m = \nabla \cdot \left(\underset{\sim}{\kappa}_m \cdot \nabla T_m \right) + q_m . \tag{6}$$

In the above equations, $\vec{V} = (u, v, w)$ is the velocity vector, p is the pressure, T is the temperature, q is the constant heat source and κ is the thermal diffusivity, μ is the fluid viscosity, α is the thermal expansion coefficient, ϕ is the porosity of the porous medium, A is the ratio of heat capacities and ρ_0 is the reference fluid density, while $\underset{\sim}{K}$ and $\underset{\sim}{\kappa}_m$ are respectively the tensors of permeability and effective thermal diffusivity which are given by $\underset{\sim}{K} = K_h(\hat{i}\hat{i} + \hat{j}\hat{j}) + K_v \hat{k}\hat{k}$, $\underset{\sim}{\kappa}_m = \kappa_{mh}(\hat{i}\hat{i} + \hat{j}\hat{j}) + \kappa_{mv}\hat{k}\hat{k}$, where the subscripts h and v refer to the quantities in the horizontal and vertical directions respectively. Thus, the horizontal isotropy with coinciding principal axes of permeability and effective thermal diffusivity to the coordinate axes are hereby assumed. The subscript m refers to the value of the parameter in the porous region.

The basic state is quiescent and is of the form

International Journal of Computer & Mathematical Sciences
IJCMS
ISSN 2347 – 8527
Volume 3, Issue 1
April 2014

$$u, v, w, p, T = \left[0, 0, W_0, p_b \ z \ , T_b \ z \ \right] \tag{7}$$

$$u_m, v_m, w_m, p_m, T_m = \left[0, 0, W_0, p_{mb} \ z \ , T_{mb} \ z \ \right]. \tag{8}$$

The temperature distributions in the basic state are given by

$$T_b \ z = T_0 + \frac{q\,d}{W_0}\left[\left(\frac{z}{d} + \frac{1-e^{W_0 z/\kappa}}{e^{W_0 d/\kappa}-1}\right)\right] - \ T_0 - T_u \ \left(\frac{1-e^{W_0 z/\kappa}}{e^{W_0 d/\kappa}-1}\right), 0 \le z \le d \tag{9}$$

$$T_{mb} \ z_m = T_0 + \frac{q_m d_m}{W_0}\left[\left(\frac{z_m}{d_m} + \frac{e^{W_0 z_m/\kappa_{mv}}-1}{e^{-W_0 d_m/\kappa_{mv}}-1}\right)\right] + \ T_l - T_0 \ \left(\frac{1-e^{W_0 z_m/\kappa_{mv}}}{e^{-W_0 d_m/\kappa_{mv}}-1}\right), -d_m \le z_m \le 0 \tag{10}$$

Where T_0 is the interface temperature. It is observed that the effect of vertical throughflow is to alter the basic temperature distribution from linear to exponential with respect to vertical coordinate in both fluid and porous layers. To investigate the stability of the basic state, infinitesimal disturbances are superimposed in the form

$$\vec{V} = \vec{V}', \quad T = T_b \ z \ + \theta, \quad p = p_b(z) + p', \quad \vec{V}_m = \vec{V}_m' \tag{11}$$

$$T_m = T_{mb} \ z_m \ + \theta_m, \quad p_m = p_{mb}(z_m) + p_m'. \tag{12}$$

Following the standard linear stability analysis procedure and noting that the principle of exchange of stability holds, we arrive at the following stability equations (for details see Chen et al. 1990 and Shivakumara et al. 2011):

$$D^2 - a^2 \quad D^2 - \eta D - a^2 \ W = Ra^2\Theta \tag{13}$$

$$D^2 - PeD - a^2 \ \Theta = \left[\frac{Ns}{Pe} + (Pe + 2Ns)\frac{e^{Pe\,z}}{1-e^{Pe}}\right]W \tag{14}$$

$$\left(\frac{1}{\xi}D_m^2 - a_m^2\right)W_m = -R_m a_m^2 \Theta_m \tag{15}$$

$$D_m^2 - Pe_m D_m - \chi a_m^2 \ \Theta_m = \left[\frac{Ns_m}{Pe_m} - (Pe_m + 2Ns_m)\frac{e^{Pe_m z_m}}{1-e^{-Pe_m}}\right]W_m. \tag{16}$$

Here, W is the amplitude of perturbed vertical velocity and Θ is the amplitude of perturbed temperature, $D = d/dz$, $Pr = \nu/\kappa$ is the Prandtl number, $Pe = W_0 d/\kappa$ is the Peclet number, $R = \alpha g\ (T_0 - T_u)\ d^3/\nu\kappa$ is the Rayleigh number, $Ns = q d^2/2\kappa\ (T_0 - T_u)$ is the dimensionless heat source strength, $a = \sqrt{l^2 + m^2}$ is the overall horizontal wave number and $\nabla^2 = \nabla_h^2 + \partial^2/\partial z^2$ is the Laplacian operator with $\nabla_h^2 = \partial^2/\partial x^2 + \partial^2/\partial y^2$. The corresponding quantities for the porous region are W_m, Θ_m, $D_m = d/dz_m$, $Pr_m = \nu/\kappa_{mv} = Pr\,\varepsilon_T$, $Pe_m = W_0 d_m/\kappa_{mv} = Pe\ \varepsilon_T/\zeta$, $R_m = \alpha g\ (T_l - T_0)\ d_m K_v/\nu\kappa_{mv} = RDa\zeta^{-4}\varepsilon_T^2$, $Ns_m = q_m d_m^2/2\kappa_{mv}\ (T_l - T_0)$, $a_m = \sqrt{\tilde{l}^2 + \tilde{m}^2}$ and $\nabla_m^2 = \nabla_{mh}^2 + \partial^2/\partial z_m^2$ with $\nabla_{mh}^2 = \partial^2/\partial x_m^2 + \partial^2/\partial y_m^2$. Further, $Da = K_v/d_m^2$ is the Darcy number, $\xi = K_h/K_v$ is the mechanical anisotropy parameter, $\chi = \kappa_{mh}/\kappa_{mv}$ is the thermal anisotropy parameter, $\varepsilon_T = \kappa/\kappa_{mv}$ is the ratio of thermal diffusivities and $\eta = Pe/Pr$ is a nondimensional group.

The boundary conditions are:

$$W = D\Theta = DW = 0 \qquad at\ z = 1 \tag{17}$$

$$W_m = D_m\Theta_m = 0 \qquad at\ z_m = -1. \tag{18}$$

At the interface (i.e., z = 0) the continuity of velocity, temperature, heat flux, normal stress and the Beavers and Joseph (1967) slip conditions are imposed. Accordingly, the conditions are:

$$W = \frac{\zeta}{\varepsilon_T} W_m,\ \Theta = \frac{\varepsilon_T}{\zeta}\Theta_m,\ D\Theta = D_m\Theta_m, \tag{19}$$

$$\left[D^2 - \eta D - 3a^2\right] DW = \frac{-\zeta^4}{\varepsilon_T Da\xi} D_m W_m \tag{20}$$

$$\left[D^2 - \frac{\beta\zeta}{\sqrt{Da\xi}} D\right] W = \frac{-\beta\zeta^3}{\varepsilon_T\sqrt{Da\xi}} D_m W_m \tag{21}$$

where $\zeta = d/d_m$ is the ratio of fluid layer to porous layer thickness and β is the Beavers-Joseph slip parameter. Thus, the problem is reduced to an eigen value problem consisting of a sixth

International Journal of Computer & Mathematical Sciences
IJCMS
ISSN 2347 – 8527
Volume 3, Issue 1
April 2014

order ordinary differential equation in the fluid layer and a fourth order ordinary differential equation in the porous layer, subject to 10 boundary conditions. If matching of the solutions in the two layers is to be possible, the wave numbers must be the same for the fluid and porous layers, so that we have $a/d = a_m/d_m$ and hence $\zeta = a/a_m$.

3 Solution by regular perturbation technique

Since the critical wave number is exceedingly small for the assumed temperature boundary conditions (Nield and Bejan 2006), the eigen value problem is solved using a regular perturbation technique with wave number $a$as a perturbation parameter. Accordingly, the dependent variables are expanded in powers of a^2in the form

$$W,\Theta = \sum_{i=0}^{N} a^{2\,i}\; W_i,\Theta_i \tag{22}$$

$$W_m,\Theta_m = \sum_{i=0}^{N}\left(\frac{a^2}{\zeta^2}\right)^i W_{mi},\Theta_{mi} \tag{23}$$

Substitution of Eqs. (22) and (23) into Eqs. (13) – 16 and the boundary conditions (17) – 21 yields a sequence of equations for the unknown functions $W_i(z),\Theta_i(z),W_{mi}(z_m)$ and $\Theta_{mi}(z_m)$ for $i = 0,1,2,3.....$.

At the leading order in a^2 Eqs. (13) – 16 become, respectively,

$$D^4W_0 - \eta D^3W_0 = 0 \tag{24}$$

$$D^2\Theta_0 - PeD\Theta_0 = W_0 f(z) \tag{25}$$

$$D_m^2W_{m0} = 0 \tag{26}$$

$$D_m^2\Theta_{m0} - Pe_m D_m\Theta_{m0} = W_{m0}g(z_m) \tag{27}$$

where

International Journal of Computer & Mathematical Sciences
IJCMS
ISSN 2347 – 8527
Volume 3, Issue 1
April 2014

$$f(z)=\frac{2Ns}{Pe}+\frac{Pe+2Ns}{1-e^{Pe}}e^{Pez}$$
$$g(z_m)=\frac{2Ns_m}{Pe_m}-\frac{Pe_m+2Ns_m}{1-e^{-Pe_m}}e^{Pe_m z_m} \quad (28)$$

and the boundary conditions $(17)-21$ become

$$W_0=0,\quad D\Theta_0=0,\quad DW_0=0 \qquad at \quad z=1 \quad (29)$$

$$W_{m0}=0,\quad D_m\Theta_{m0}=0, \qquad at \quad z_m=-1. \quad (30)$$

And at the interface$(i.e\ z=0)$

$$W_0=\frac{\zeta}{\varepsilon_T}W_{m0},\ \Theta_0=\frac{\varepsilon_T}{\zeta}\Theta_{m0},\ D\Theta_0=D_m\Theta_{m0} \quad (31)$$

$$D^3W_0-\eta D^2W_0=\frac{-\zeta^4}{Da\xi\varepsilon_T}D_mW_{m0} \quad (32)$$

$$D^2W_0-\frac{\beta\zeta}{\sqrt{Da\xi}}DW_0=\frac{-\beta\zeta^3}{\varepsilon_T\sqrt{Da\xi}}D_mW_{m0}. \quad (33)$$

The solution to the zeroth order Eqs. $(24)-(27)$ is given by

$$W_0=0,\quad \Theta_0=\frac{\varepsilon_T}{\zeta},\ W_{n0}=0,\quad \Theta_{m0}=1. \quad (34)$$

At the first order in a^2 Eqs. $(13)-(16)$ then reduce to

$$D^4W_1-\eta D^3W_1=R\frac{\varepsilon_T}{\zeta} \quad (35)$$

$$D^2\Theta_1-Pe\,D\Theta_1=W_1\,f(z)+\frac{\varepsilon_T}{\zeta} \quad (36)$$

$$D_m^2W_{m1}=-\xi R_m \quad (37)$$

$$D_m^2\Theta_{m1}-Pe_mD_m\Theta_{m1}=W_{m1}\,g(z_m)+\chi \quad (38)$$

and the boundary conditions $(17)-21$ become

International Journal of Computer & Mathematical Sciences
IJCMS
ISSN 2347 – 8527
Volume 3, Issue 1
April 2014

$$W_1 = 0, \quad D\Theta_1 = 0, \quad DW_1 = 0 \qquad at \quad z = 1 \tag{39}$$

$$W_{m1} = 0, \quad D_m\Theta_{m1} = 0, \qquad at \quad z_m = -1. \tag{40}$$

And at the interface$(i.e\ z = 0)$

$$W_1 = \frac{1}{\zeta\varepsilon_T} W_{m1}, \ \Theta_1 = \frac{\varepsilon_T}{\zeta^3}\Theta_{m1}, \ D\Theta_1 = \frac{1}{\zeta^2} D_m\Theta_{m1} \tag{41}$$

$$D^3W_1 - \eta D^2W_1 = \frac{-\zeta^2}{Da\xi\varepsilon_T} D_m W_{m1} \tag{42}$$

$$D^2W_1 - \frac{\beta\zeta}{\sqrt{Da\xi}} DW_1 = \frac{-\beta\zeta}{\varepsilon_T\sqrt{Da\xi}} D_m W_{m1}. \tag{43}$$

The general solutions of Eq. (25) and (27) are respectively given by

$$W_1 = R\left[C_1 + C_2 z + C_3 z^2 + C_4 e^{\eta z} - \frac{Da\,\varepsilon_T^3}{6\eta\zeta} z^3 \right] \tag{44}$$

$$W_{m1} = R\left[C_5 + C_6 z_m - \frac{\xi Da\,\varepsilon_T^2}{2\zeta^4} z_m^2 \right] \tag{45}$$

where

$$C_1 = \left(\frac{C_2}{\varepsilon_T\xi} - C_4 \right), \ C_2 = \left(\frac{\xi\varepsilon_T}{\zeta} - \frac{C_1}{2\xi} - C_3 - e^{\eta} C_4 \right), \ C_3 = \frac{b_{10} + b_9 C_6}{b_4}, \ C_4 = \frac{b_6\varepsilon_T\zeta - \varepsilon_T\zeta C_3 + C_3}{\xi C_1}$$

$$C_5 = \frac{C_1}{2\zeta(1+2\xi)} + C_6, \ b_1 = \left(\frac{2\zeta^2\sqrt{Da}}{2\xi} + \beta\zeta^3 \right) b_2 = \ \eta^2\zeta^2\sqrt{Da\xi} - \beta\zeta^3\eta \ - \beta\zeta^3 \ \sqrt{Da\xi} - e^{\eta} \ ,$$

$$b_3 = \left(\Delta_2\sqrt{Da\xi} - \frac{\beta\zeta^3}{\varepsilon_T\zeta} \right), \ b_4 = \left(\frac{\varepsilon_T\beta\zeta^3}{6\eta\zeta} - \frac{\beta\zeta^3\sqrt{Da\xi}}{\varepsilon_T\zeta} \right), b_5 = \ \eta - 1 \ e^{\eta} + \sqrt{Da\xi},$$

International Journal of Computer & Mathematical Sciences
IJCMS
ISSN 2347 – 8527
Volume 3, Issue 1
April 2014

$$b_6 = \left(\frac{2\varepsilon_T}{6\eta\zeta} - \frac{\sqrt{Da\xi}}{\varepsilon_T \zeta} \right), \; b_7 = \left(b_1 b_3 - \frac{b_2}{\varepsilon_T \zeta} \right), \; b_8 = \left(b_3 b_5 - \frac{b_2}{\varepsilon_T \zeta} \right), \; b_9 = \; b_4 b_5 + 2 b_7 b_6 \;\; ,$$

$$b_{10} = \frac{b_1 b_7 - b_8 b_6}{\left(b_1 b_7 - \frac{b_4}{\varepsilon_T \zeta} \right)},$$

Equations (36) and (38) involving $D^2\Theta_1$ and $D_m^2\Theta_{m1}$ respectively provide the solvability requirement which is given by

$$\int_0^1 f(z) W_1 \, dz + \frac{\chi}{\zeta^2} \int_{-1}^0 g(z_m) W_{m1} \, dz = -\frac{\varepsilon_T}{\zeta} - \frac{\chi}{\zeta^2} \qquad (46)$$

In the absence of throughflow (i.e.,$Pe \to 0$), both the functions $f(z)$ and $g(z_m)$ take the value -1 and the above condition reduces to that of Nield (1977).

The expressions for W_1 and W_{m1} are back substituted into Eq. (53) and integrated to yield an expression for the critical Rayleigh number R_m^c, which is given by

$$R_m^c = \frac{-\left(\frac{\varepsilon_T}{\zeta} + \frac{\chi}{\zeta^2} \right) \left(\frac{Da\, \varepsilon_T^2}{\zeta^4} \right)}{\delta_1 C_1 + \delta_2 C_2 + \delta_3 C_3 + \delta_4 C_4 + \delta_5 \; + \frac{\chi}{\zeta^2} \; - C_5 + \delta_6 C_6 - \delta_3 \delta_7} \qquad (47)$$

where

$$\delta_1 = \left(\frac{4Ns}{Pe} + 1 \right), \;\; \delta_3 = \left[\frac{2Ns}{3Pe} + \frac{Pe + 2Ns}{1 - e^{Pe}} \left(\frac{e^{Pe}}{Pe} - \frac{2e^{Pe}}{Pe^2} + \frac{2\;1 - e^{Pe}}{Pe^3} \right) \right]$$

$$\delta_4 = \left[\frac{2Ns}{\eta Pe} + \frac{Pe + 2Ns}{1 - e^{Pe}} \frac{e^{\,Pe+\eta} \; - 1}{Pe + \eta} \right]$$

$$\delta_5 = -\frac{\varepsilon_T}{6\eta\zeta} \left[\frac{2Ns}{Pe} + \frac{Pe + 2Ns}{1 - e^{Pe}} \left(\frac{e^{Pe}}{Pe} - \frac{3e^{Pe}}{Pe^2} + \frac{6e^{Pe}}{Pe^3} + \frac{6\;\; e^{Pe} - 1}{Pe^4} \right) \right]$$

International Journal of Computer & Mathematical Sciences
IJCMS
ISSN 2347 – 8527
Volume 3, Issue 1
April 2014

$$\delta_6 = \left[\frac{-Ns_1}{Pe_m} + \frac{Pe_m + 2Ns_1}{1-e^{-Pe_m}} \left(\frac{-e^{-Pe_m}}{Pe_m} - \frac{e^{-Pe_m}-1}{Pe_m^2} \right) \right], \quad \delta_7 = \left[\frac{2Ns_1}{3Pe_m} + \frac{e^{-Pe_m}}{Pe_m} + \frac{2e^{-Pe}}{Pe_m^2} + \frac{2\ e^{-Pe_m}-1}{Pe_m^3} \right].$$

The expression for R_m^c is evaluated for different values of various physical parameters and the results are discussed in detail in the next section

4 Results and Discussion

The onset of penetrative convection via internal heating in the presence of a vertical throughflow is considered in a system consisting of a fluid layer overlying a anisotropic porous layer. In the calculation, we have chosen the value of $\phi = 0.389$, C_b=209.25 and $\sqrt{Da} = 3.04 \times 10^{-3}$ which correspond to 3 cm deep porous layer consisting of 3mm diameter glass beads (Chen, 1990). The results are discussed for different values of depth ratios ζ .The following three different cases of internal heating pattern is considered for discussion namely,

Case (i): internal heat source in the porous layer alone (i.e., $Ns_f = 0$, $Ns_m = 5$)

Case (ii): internal heat sources in both fluid and porous layers(i.e., $Ns_f = 5$, $Ns_m = 5$) and

Case (iii): internal heat source in the fluid layer alone (i.e., $Ns_f = 5$, $Ns_m = 0$).

International Journal of Computer & Mathematical Sciences
IJCMS
ISSN 2347 – 8527
Volume 3, Issue 1
April 2014

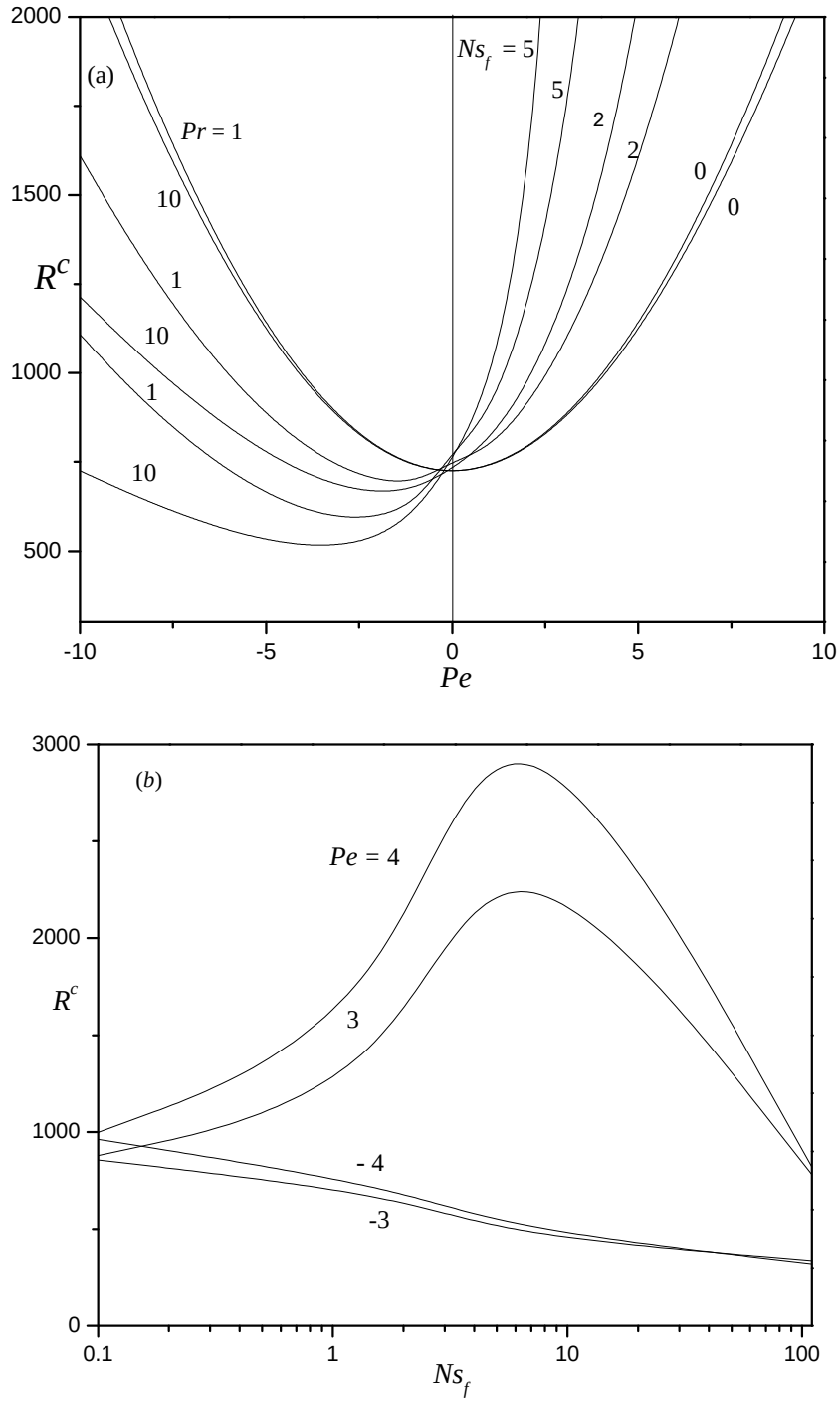

Fig. 2. Critical Rayleigh number versus (a) Pe for two values of Pr and Ns_f, (b) Ns_f for different values of Pe with $Pr = 10$ (single fluid layer case, $\zeta >> 1$)

International Journal of Computer & Mathematical Sciences
IJCMS
ISSN 2347 – 8527
Volume 3, Issue 1
April 2014

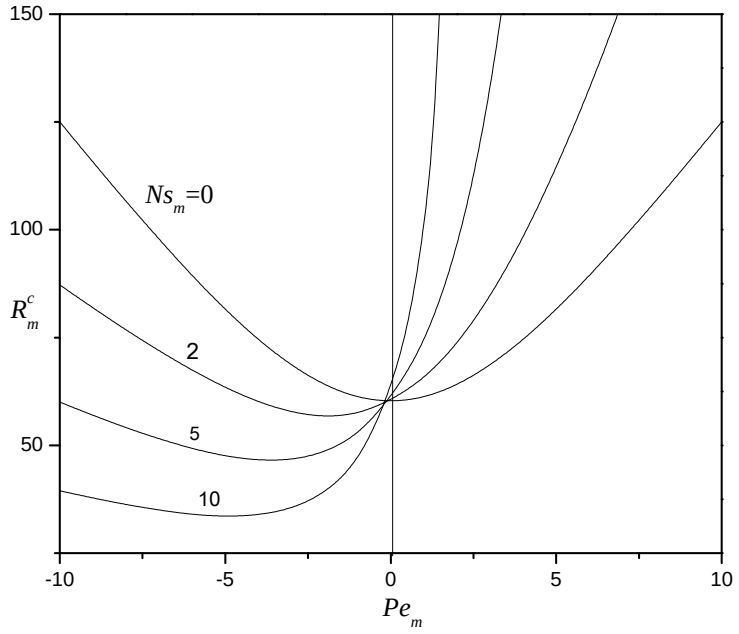

Fig. 3. Critical Rayleigh number versus Pe_m for different values of Ns_m when $\xi = 0.1$ and χ=0.5 ,(single fluid layer case, $\zeta << 1$)

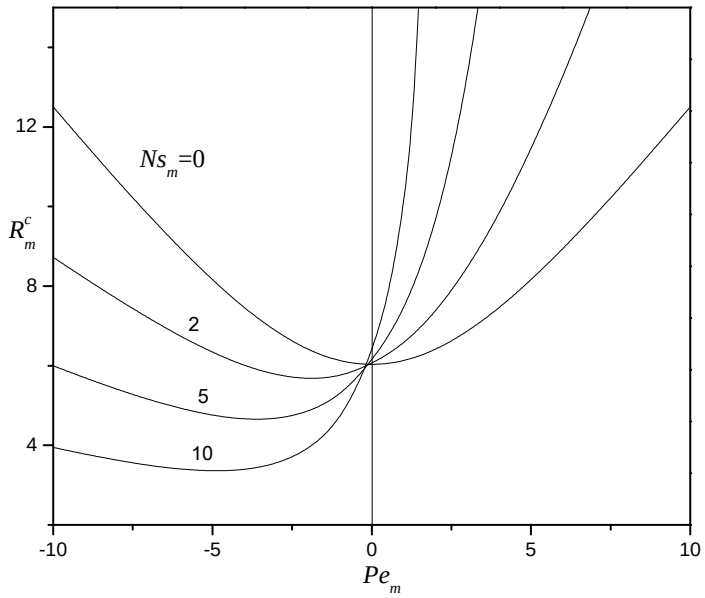

Fig. 4. Critical Rayleigh number versus Pe_m for different values of Ns_m when $\xi = 1$ and χ=0.5 (single fluid layer case, $\zeta << 1$)

International Journal of Computer & Mathematical Sciences
IJCMS
ISSN 2347 – 8527
Volume 3, Issue 1
April 2014

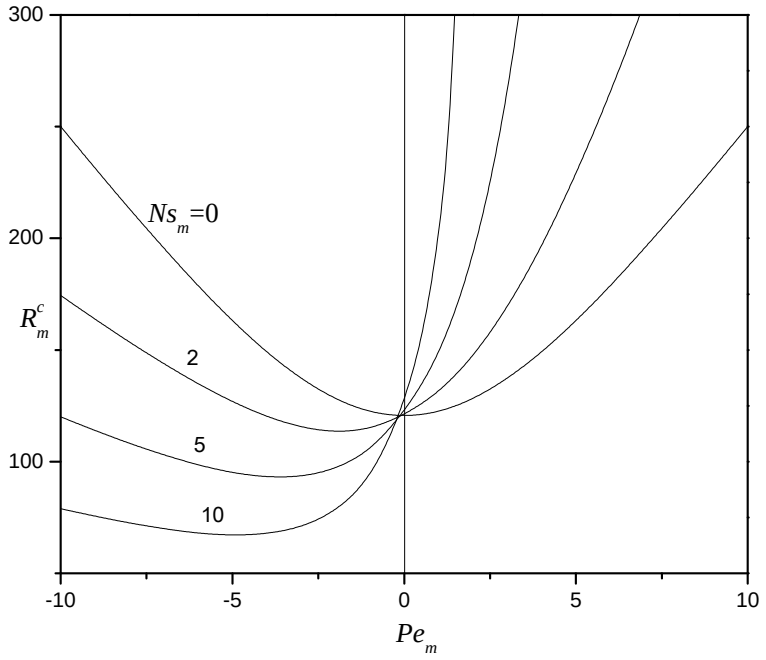

Fig. 5. Critical Rayleigh number versus Pe_m for different values of Ns_m when $\xi = 0.1$ and χ=1 (single fluid layer case, $\zeta << 1$)

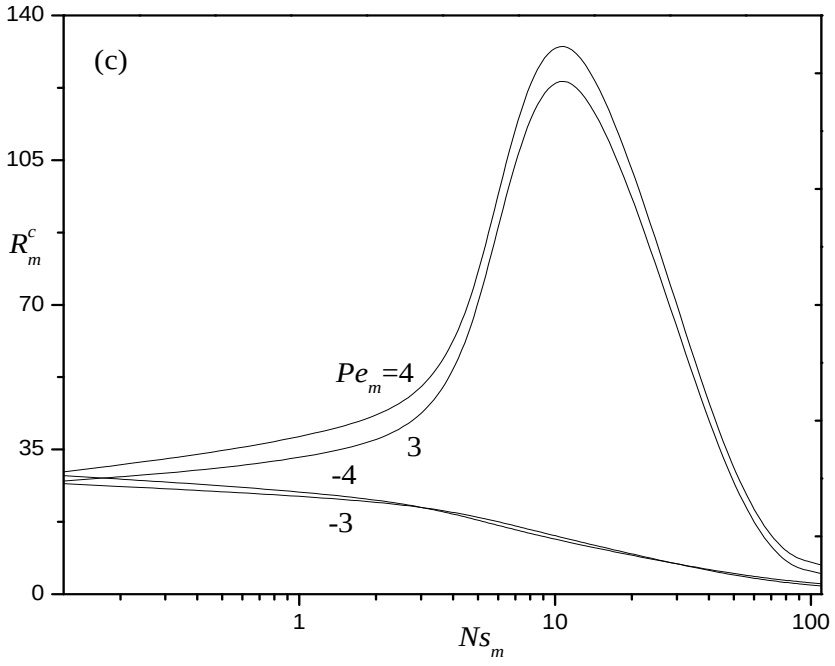

International Journal of Computer & Mathematical Sciences
IJCMS
ISSN 2347 – 8527
Volume 3, Issue 1
April 2014

Fig. 6. Critical Rayleigh number versus Ns_m for different values of Pe_m with $Ns_f = 0$ when $\xi = 0.5$ and χ=0.5 (single fluid layer case, $\zeta << 1$)

4.1 Depth ratio $\zeta >> 1$

This is the case of a pure fluid layer and the stability characteristic of the system is measured by the Rayleigh number R. When $Ns_f = 0$ and $Pe = 0$, the known exact value $R^c = 720$ (Sparrow et al.1964) is retrieved. The direction of throughflow has no influence on the stability of the system in the absence of internal heating and throughflow is to delay the onset of convection. This may be attributed to the fact that the primary effect of throughflow is to confine significant thermal gradients to a thermal boundary layer at the boundary toward which the throughflow is directed. The effective length scale is thus smaller than the layer thickness d and hence the effective Rayleigh number which will be depending on d^3 will be much less than the actual Rayleigh number. A larger value of Rayleigh number is thus necessary to initiate the convection. Nonetheless, the simultaneous presence of throughflow and internal heating alters the basic temperature distribution so that the direction of throughflow also affects the stability of the system. As a result of this some unusual behaviors are observed namely, (i) downward throughflow initially shows some destabilizing effect (Fig. 2a) and (ii) increasing internal heat source strength causes stabilizing effect for upward throughflow initially (Fig. 2b).

The presence of throughflow brings in the effect of Prandtl number Pr on the characteristics of stability of the system. Increasing the value of Prandtl number is to hasten the onset of convection in the absence of internal heating but the variation in the critical Rayleigh number R^c for Pr =1 and 10 is found to be not so significant. In the presence of internal heating, however, the effect of increasing Pr is destabilizing for only downward throughflow and an opposite behavior is noticed for upward throughflow. Besides, R^c for Pr =1 and 10 are not close in the presence internal heating. The upward throughflow is found to be more stabilizing than downward throughflow.

International Journal of Computer & Mathematical Sciences
IJCMS
ISSN 2347 – 8527
Volume 3, Issue 1
April 2014

4.2 Depth ratio $\zeta << 1$

In the absence of internal heating ($Ns_m = 0$) and throughflow ($Pe_m = 0$), we recover the known exact value $R_m^c = 12$ (Nield and Bejan 2006) for pure isotropic porous layer ($\xi = 1 = \chi$).

In the case anisotropic porous layer it is observed that the direction of throughflow matters only in the presence of internal heating. Figures 3 - 6 it is noted that R_m^c attains higher values at lower values of ξ for the absence and presence of internal heating. That is, decrease in the mechanical anisotropy parameter is to delay the onset of convection. This is because, decrease in ξ corresponds to smaller horizontal permeability which in turn hinder the motion of fluid in the horizontal direction. As a consequence, the conduction process in the porous medium becomes more stable and hence higher values of R_m^c are needed for the onset of convection and Figures 3 - 6 illustrate that the results are qualitatively similar to those of $\zeta >> 1$.

4.3 Depth ratio $\zeta = 1$

The stability of the system is characterized by R_m^c. Figure 7 exhibit plots of R_m^c as a function of $\mathrm{P}e_m$ respectively for the above mentioned three cases of internal heating pattern for $\xi = 0.5, \chi = 0.5$. The results are presented for two values of Prandtl number $Pr = 1$ and 100. From Fig. 7 it is seen that for all values of Pr for the case of internal heating porous layer stabilizes the system both upward and downward throughflow. And upward throughflow shows stabilizing effect for other two combination heating layer ($Ns_f = 5, Ns_f = 5$ and $Ns_f = 5, Ns_f = 0$) and for downward through flow the system is destabilizing when $-3.5 \le Pe_m \le 0$, and $-4.2 \le Pe_m \le 0$ for Pr = 1 and 100, respectively and for higher values of Pe_m the system is stabilizing. For Pr =0.1, the system is always stabilizing as the value of R_m^c increases with Pe_m.

International Journal of Computer & Mathematical Sciences
IJCMS
ISSN 2347 – 8527
Volume 3, Issue 1
April 2014

Figure 8 exhibit plots of R_m^c as a function of $\mathrm{P}e_m$ for different values of ξ. The results are presented for $\chi = 0.5$, $\mathrm{Pr} = 10$ for the above mentioned three cases of internal heating pattern. From Fig. 8 it is seen that for all values of ξ for the case of internal heating porous layer stabilizes the system both upward and downward throughflow and for other two combination heating layer ($Ns_f = 5$, $Ns_f = 5$ and $Ns_f = 5$, $Ns_f = 0$) and for downward through flow the system is destabilizing when $-3.8 \le Pe_m \le 0$ for all values of ξ and stabilizes the system for upward through flow. Hence the system is more stabilizing for decreasing the values of ξ.

Figure 9 exhibit plots of R_m^c as a function of $\mathrm{P}e_m$ for different values of χ . The results are presented for $\xi = 0.5$, $\mathrm{Pr} = 10$ for the above mentioned three cases of internal heating pattern. From Fig. 9 it is seen that for all values of χ for the case of internal heating porous layer stabilizes the system both upward and downward throughflow and for other two combination heating layer ($Ns_f = 5$, $Ns_f = 5$ and $Ns_f = 5$, $Ns_f = 0$) and for downward through flow the system is destabilizing when $-3.4 \le Pe_m \le 0$ for all values of ξ and stabilizes the system for upward through flow. Hence the system is more stabilizing for increasing the values of χ.

International Journal of Computer & Mathematical Sciences
IJCMS
ISSN 2347 – 8527
Volume 3, Issue 1
April 2014

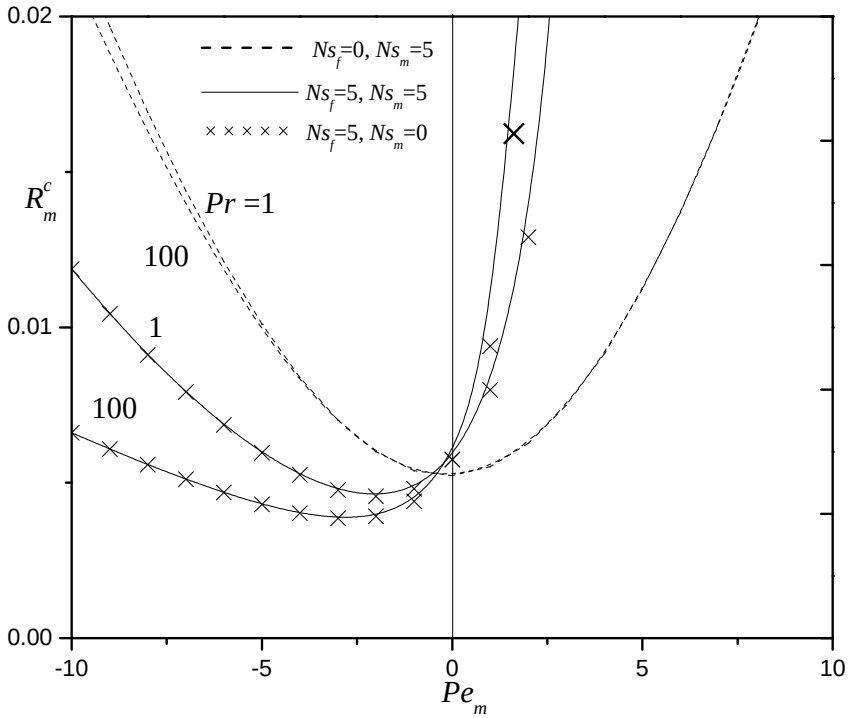

Fig. 7. Critical Rayleigh number versus Peclet number for different values of Pr and Ns_f, Ns_m for $\xi = 0.5$, $\chi = 0.5$ and $\zeta = 1$.

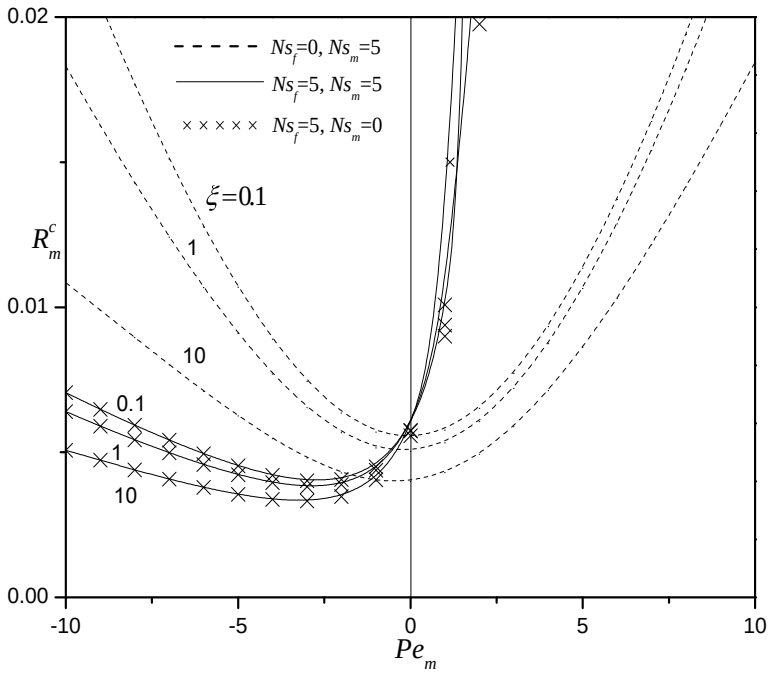

Fig. 8. Critical Rayleigh number versus Peclet number for different values of ξ and

International Journal of Computer & Mathematical Sciences
IJCMS
ISSN 2347 – 8527
Volume 3, Issue 1
April 2014

Ns_f , Ns_m for $\chi = 0.5, \Pr = 10, \zeta = 1.$

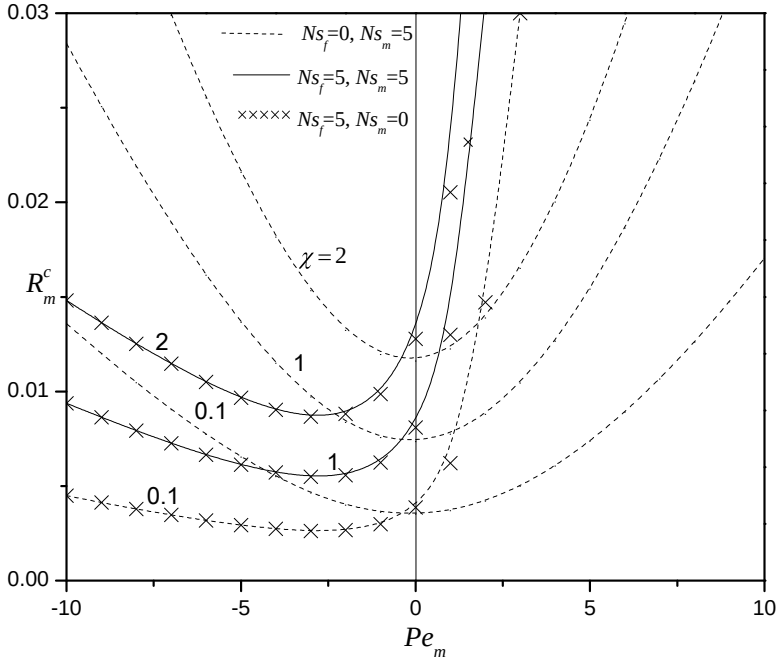

Fig. 9. Critical Rayleigh number versus Peclet number for different values of χ and Ns_f , Ns_m for $\xi = 0.5, \Pr = 10, \zeta = 1.$

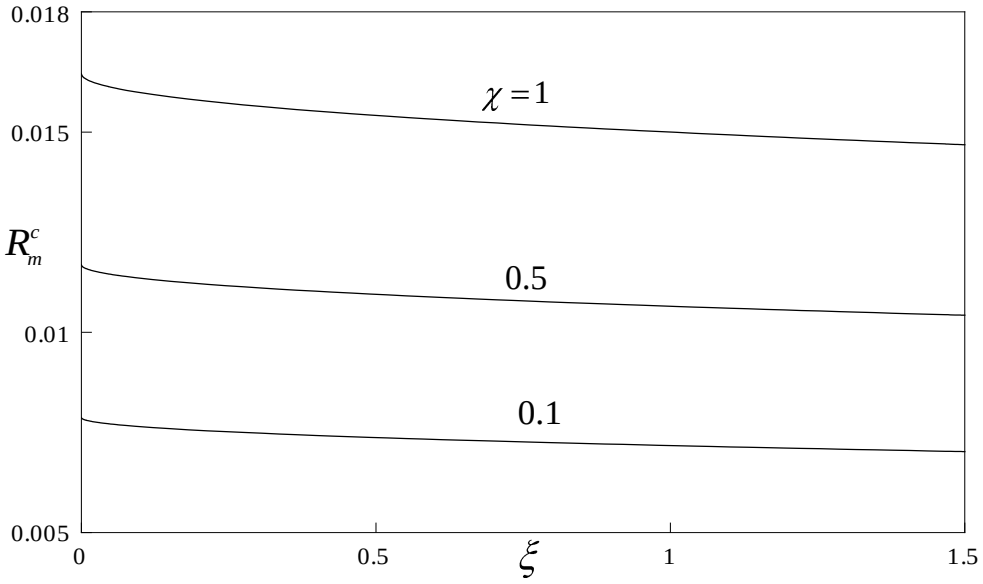

Fig. 10. Critical Rayleigh number versus ξ for different values of χ for $Ns_f = 0, Ns_m = 2, \Pr = 1, \zeta = 1.$

International Journal of Computer & Mathematical Sciences
IJCMS
ISSN 2347 – 8527
Volume 3, Issue 1
April 2014

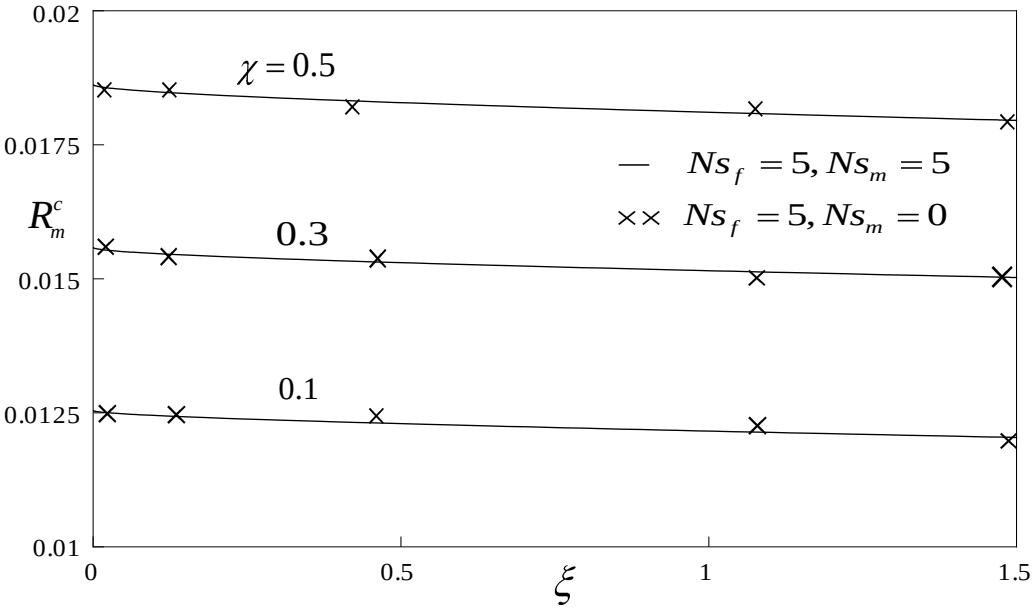

Fig. 11. Critical Rayleigh number versus ξ for different values of χ and Ns_f , Ns_m for $\Pr = 1, \zeta = 1.$

The effect of mechanical and thermal anisotropic parameters on the onset of convection is emphasized by depicting the variation of R_m^c and over a range of mechanical anisotropy parameter ξ for different values of thermal anisotropy parameter χ in Figs. 10 and 11, respectively for a fixed value of $Pr = 1, \zeta = 1.$ It is observed that R_m^c increases with the decreasing ξ. Physically, this means that the conduction solution in the porous medium becomes more stable and the critical wavelength decreases as the horizontal permeability decreases. Smaller horizontal permeability inhibits horizontal motion, and the conduction solution is thus stabilized. The larger resistance to horizontal flow also leads to a shortening of the horizontal wavelength at onset. In the same figure, it is seen that for a given and smaller values of the horizontal thermal diffusivity correspond to destabilization of the basic state, and the onset of convection at a smaller wavelength, This can be explained by the fact that as χ decreases, a

International Journal of Computer & Mathematical Sciences
IJCMS
ISSN 2347 – 8527
Volume 3, Issue 1
April 2014

heated fluid parcel loses less heat in the horizontal directions, and hence retains its buoyancy better. Therefore, the base state becomes less stable, and the wavelength is reduced.

5 Conclusions

The criterion for the onset of penetrative convection in an anisotropic porous layer underlain by a fluid layer is investigated theoretically to understand control of penetrative convection. The Forchheimer-extended Darcy equation is used in the porous medium and the Beavers–Joseph slip condition is applied at the interface between the fluid and the porous layers. The boundaries are considered to be rigid, however permeable, and insulated to temperature perturbations. The resulting eigen value problem is solved by regular perturbation technique. From the foregoing analysis, it is observed that the stability characteristics of the configuration depend crucially on (i) the presence of internal heating in fluid and/or porous layer, (ii) depth ratio ζ, (iii) mechanical anisotropy parameter ξ, (v) thermal anisotropy parameter χ, and (vi) throughflow direction. For ζ =1, the system is more stabilizing if the porous layer alone is heated internally as compared to other two types of heating pattern. Decreasing the mechanical anisotropy parameter ξ and increasing the thermal anisotropy parameter χ, the system is stabilizing.

Acknowledgments The authors Y. H. Gangadharaiah, S. P. Suma, and H. Nagarathnamma wish to express their thanks to the management of their respective colleges for the encouragement.

References

Allen MB. Collocation techniques for modeling compositional flows in oil reservoirs. Springer; 1984.

Beavers, G.S., Joseph, D.D.: Boundary conditions at a naturally permeable wall, J. Fluid Mech. 30, 197–207(1967)

Chen, F.: Throughflow effects on convective instability in superposed fluid and porous Layers.J. Fluid. Mech.231, 113–133(1990)

International Journal of Computer & Mathematical Sciences
IJCMS
ISSN 2347 – 8527
Volume 3, Issue 1
April 2014

Carr, M, Straughan, B.: Penetrative convection in a fluid overlying a porous medium. Adv.Water Resour. 26, 262–276 (2003)

Carr, M.: Penetrative convection in a superposed porous- medium–fluid layer via internal heating. J. Fluid Mech. 509, 305–329 (2004)

Hill, A.A., Straughan, B.: Poiseuille flow in a fluid overlying a highly porous material. Adv. Water Resour.**32**, 1609–1614 (2009)

Khalili, A., Shivakumara., I.S, Suma, S.P.: Convective instability in superposed fluid and porous layers with vertical throughflow. Transp. Porous Med. 51, 1–18(2003)

Nield, D.A, Bejan A.: Convection in Porous Media. Second ed. Springer-Verlag. New York(2006)

Nield, D.A.: Onset of convection in a fluid layer overlying a layer of a porous medium. J. Fluid Mech. **81**,513–522 (1977)

Shivakumara, I. S., Suma, S. P., Indira, R., Gangadharaiah, Y. H.: Effect of internal heat generation on the onset of Marangoni convection in a fluid layer overlying a layer of an anisotropic porous medium. Transp. Porous Med. Vol.92, pp.727-743, 2012.

Shivakumara, I.S, Jinho, L., Chavaraddi, K.B.: Onset surface tension convection in a fluid layer overlying a layer of an anisotropic porous medium. Int. J. Heat Mass Transf. **54**, 994–1001 (2011)

Sparrow, E.M., Goldstin, R.J., Jonssn, V.K.: Thermal instability in horizontal fluid layer: effect of boundary conditions and non-linear temperature. J. Fluid Mech. **18**, 513–529 (1964)